



# HMCES safeguards replication from oxidative stress and ensures error-free repair

Mrinal Srivastava, Dan Su , Huimin Zhang , Zhen Chen, Mengfan Tang, Litong Nie & Junjie Chen\* 

## Abstract

Replication across oxidative DNA lesions can give rise to mutations that pose a threat to genome integrity. How such lesions, which escape base excision repair, get removed without error during replication remains unknown. Our PCNA-based screen to uncover changes in replisome composition under different replication stress conditions had revealed a previously unknown PCNA-interacting protein, HMCES/C3orf37. Here, we show that HMCES is a critical component of the replication stress response, mainly upon base misincorporation. We further demonstrate that the absence of HMCES imparts resistance to pemetrexed treatment due to error-prone bypass of oxidative damage. Furthermore, based on genetic screening, we show that homologous recombination repair proteins, such as CtIP, BRCA2, BRCA1, and PALB2, are indispensable for the survival of HMCES KO cells. Hence, HMCES, which is the sole member of the SRAP superfamily in higher eukaryotes known so far, acts as a proofreader on replication forks, facilitates resolution of oxidative base damage, and therefore ensures faithful DNA replication.

**Keywords** antimetabolite inhibitors; base excision repair; oxidative damage; replication stress; translesion synthesis

**Subject Categories** DNA Replication, Repair & Recombination

**DOI** 10.15252/embr.201949123 | Received 21 August 2019 | Revised 14 March 2020 | Accepted 19 March 2020 | Published online 19 April 2020

**EMBO Reports (2020) 21: e49123**

## Introduction

DNA replication is a tightly regulated process that ensures accurate transfer of genetic information. This complex process not only involves duplication of genome but also coordinates maintenance of epigenetic regulation, which ensures faithful transmission of genetic information [1,2]. PCNA, a replication clamp, has been shown to regulate these processes via a variety of specific protein interactions [3]. Ongoing replication fork devises numerous measures to safeguard fidelity and success of replication upon encountering various DNA lesions. One of the most common types of DNA lesions are generated through exposure to reactive oxygen species (ROS),

resulting from exogenous and endogenous processes. ROS can create base and sugar damage, apurinic/aprimidinic (AP) or abasic sites, strand breaks, or DNA–protein crosslinks [4]. Several pro-mutagenic oxidation products such as 8-oxo-7,8-dihydro-2'-deoxyguanosine (8-oxodG) and 8-oxo-7,8-dihydro-2'-deoxyadenosine (8-oxodA) are products of guanine and adenine, respectively [5]. Oxidation of pyrimidines can give rise to thymine glycol (Tg) and 5-hydroxycytosines [5]. Error-free repair of these oxidized bases is crucial for maintaining genome integrity, which is achieved mainly by base excision repair (BER) [6]. However, some of these base lesions may evade cellular repair pathways and lead to mutations, especially in S phase cells. For example, although 8-oxodG is not a fork-blocking lesion, it is often misrecognized by replicative polymerases ( $\alpha$ ,  $\delta$ ,  $\epsilon$ ) and forms Hoogsteen base pairing with adenine, which results in CG to AT transversion mutation [7,8]. Tg, due to their resultant structural changes and non-planar geometry, not only pose as fork-blocking lesions but also confer extension impairment for replicative polymerases [9]. AP site can also be generated as an intermediate of BER pathway, which acts as a non-instructive DNA lesion for polymerases, and, in mammalian cells, adenine is often misincorporated opposite an AP site by translesion synthesis (TLS) polymerases [10].

The actions of these repair pathways have been explored meticulously to create various chemotherapeutic regimes. Thymidylate synthase inhibitors, 5-fluorouracil (5-FU) and pemetrexed that exploit BER pathway, are front-line therapeutic agents for solid cancers especially for the treatment for colorectal and lung cancer, respectively [11,12]. Their actions lead to an imbalanced nucleotide pool in cells, resulting in misincorporation of dUTP in the DNA along with 5-fluoro-2'-dUTP, in case of 5-FU treatment. All the known repair pathways correct such damaged bases either before or after replication [13]. How cells maintain the fidelity of repair when the replication fork encounters such lesions is largely unknown.

Recently, we and others have identified HMCES as a protein important for replication stress response [1,14]. Here, we report that HMCES, which is an evolutionally conserved DNA repair protein, interacts with PCNA on replication fork. We show that HMCES plays an important role in oxidative stress response in cells. We propose that HMCES may therefore act as a proofreading enzyme that helps in resolution of mutagenic sites by propelling them toward BER repair. In the absence of HMCES, such lesions are

repaired through error-prone TLS. Furthermore, we show that HMCES deficiency imparts synthetic lethality toward loss of key homologous recombination repair (HRR) proteins.

## Results and Discussion

### HMCES is a conserved replication-associated protein

In an earlier study, we explored the PCNA interactome by using affinity purification and proximity labeling methods followed by mass spectrometry (MS) analysis under normal and replication stress conditions (Figs 1A and EV1A and B) [1]. We identified a previously unknown interacting partner of PCNA, HMCES/C3ORF37, which is a part of the replisome complex under normal conditions; however, it was further enriched upon DNA damage (Figs 1A and EV1A and B) [1]. HMCES/C3ORF37 was first identified as a reader of hydroxymethylcytosine in embryonic stem cells and belongs to an evolutionarily conserved superfamily of proteins containing DUF159/SOS response-associated peptidase (SRAP) domains, which have been shown to be responsible for SOS response in prokaryotes [15,16] (Fig EV2A and B). The SOS response network, which is stress-induced and regulates DNA repair and mutagenesis in bacteria, is very well elucidated [17]; however, its role in higher eukaryotes remains elusive. We confirmed the binding of HMCES to PCNA and, by utilizing a series of deletion mutants of the HMCES protein, we narrowed down the PCNA-binding region to its C-terminus (Fig 1B and C). *In vitro* glutathione S-transferase (GST)-PCNA pull-down experiments further confirmed this as direct interaction between PCNA and HMCES (Fig 1D). Further, we validated the presence of HMCES on replication fork using accelerated native isolation of proteins on nascent DNA (aniPOND) analysis followed by Western blotting. HMCES enriched on nascent replication fork and diminished upon chase with thymidine (Fig 1E). PCNA and RPA70 were included as positive controls (Fig 1E).

Since HMCES associates with PCNA and replisome complex, we enquired about regulation of its expression during cell cycle. CYCLIN E and CYCLIN B1 were used as controls that peak at G1/S and G2/M phase, respectively (Figs 1F and EV3A). We found that HMCES expression was not significantly regulated or restricted to any phase of the cell cycle (Figs 1F and EV3B), indicating the possibility that its function may not be limited to replication-associated roles. Alternatively, its regulation may not be achieved mainly at its expression level.

### HMCES plays a role in replication stress response

In order to explore the *in vivo* functions of HMCES, we generated HMCES knockout (HMCES KO) 293A cells using CRISPR-CAS9 technology, which were validated by Western blotting and sequencing (Figs 2A and EV4A). Compared to wild-type (WT) cells, HMCES KO cells had lower colony-forming capability (Fig 2B and C), suggesting that HMCES is important for cell proliferation. Next, we evaluated the possible role of HMCES in responding to replication stress conditions. We observed an apparent increased sensitivity of HMCES KO cells to hydroxyurea (HU) treatment (Figs 2D and E, and EV4B), suggesting a possible role of HMCES in replication stress response. shRNA-mediated knockdown of HMCES in 293A cells also displayed similar sensitivity to HU treatment (Fig EV4C and D). Cell cycle analysis showed appreciable G2/M arrest 12 h after release from HU treatment in HMCES KO cells (Fig EV4E). Furthermore, we specifically analyzed the sensitivity of HMCES KO cells to ROS-inducing, DNA-damaging agents such as ionizing radiation (IR) and H<sub>2</sub>O<sub>2</sub>. IR and H<sub>2</sub>O<sub>2</sub> treatment can result in complex DNA lesions such as oxidized bases and AP sites along with strand breaks. We found that both of these treatments conferred greater sensitivity to HMCES KO and knockdown cells than that in control wild-type cells (Figs 2F–H and EV4F). Evaluation of cell death upon H<sub>2</sub>O<sub>2</sub> treatment showed increase in both apoptotic and necrotic populations in HMCES KO cells (Fig EV4G). Further, we performed reconstitution assays with WT and various conserved site mutants of HMCES (Figs 2A and I, and EV4H and I). Reconstitution of WT HMCES was able to rescue sensitivity toward H<sub>2</sub>O<sub>2</sub> in HMCES KO cells (Fig 2I). We strategically reconstituted HMCES KO cells with a series of HMCES mutants, which affect the most evolutionarily conserved residues, to explore their involvement in DNA repair (Fig EV4H). Residues C2 and E127 have been proposed to be responsible for potential cysteine protease activity [18]. Among the mutants tested, HMCES  $\Delta$ 41–51 mutant protein showed significantly reduced stability (Fig EV4I), which contains deletion of the enzymatically relevant and conserved Ser and Tyr residues [19]. More recently, a small region (N96–98) was shown to be important for the DNA binding activity of HMCES [14]. HMCES KO cells, along with cells expressing C2A mutant protein, remained most sensitive to H<sub>2</sub>O<sub>2</sub> exposure, followed by cells expressing E127A or N96A mutants (Fig EV4H and I).

Since 8-oxodG is the most abundant type of base oxidation product in the cell owing to the lower redox potential of guanines, we assessed whether resolution of 8-oxodG is affected in HMCES KO cells. To test this possibility, cells were treated with KBrO<sub>3</sub> and

#### Figure 1. HMCES directly interacts with PCNA and is part of replisome complex.

- A Summary of HMCES recovery upon TAP-MS analyses performed with 293T cells stably expressing SFB-PCNA. Cells were treated with CPT: camptothecin (1  $\mu$ g/ml for 6 h); HU: hydroxyurea (2 mM for 16 h), UV: ultraviolet light irradiation (10 mJ/cm<sup>2</sup> harvested after 6 h post-irradiation), or thymidine (100 mM for 6 h). Recovered peptide-spectrum matches (PSMs) for PCNA and HMCES are indicated for each condition.
- B Schematic representation of HMCES domain organization and deletion mutants used in this study.
- C Immunoprecipitation (IP) of SFB-tagged full-length (FL) HMCES and indicated HMCES deletion mutants was conducted to decipher the region responsible for PCNA interaction.
- D GST-PCNA pull-down assay was used to evaluate the interaction between PCNA and full-length HMCES or indicated HMCES deletion mutants.
- E aniPOND–Western blotting analysis revealed the presence of HMCES on replication fork. Cells were pulsed with EdU for 10 min, and click reaction was performed. In thymidine chase samples, cells were incubated with thymidine for another 30 min prior to click reaction.
- F Analysis of HMCES level throughout the cell cycle. Cells were synchronized by double thymidine block and released for the indicated time points. CYCLIN E and CYCLIN B1 were used as markers for cell cycle phases.

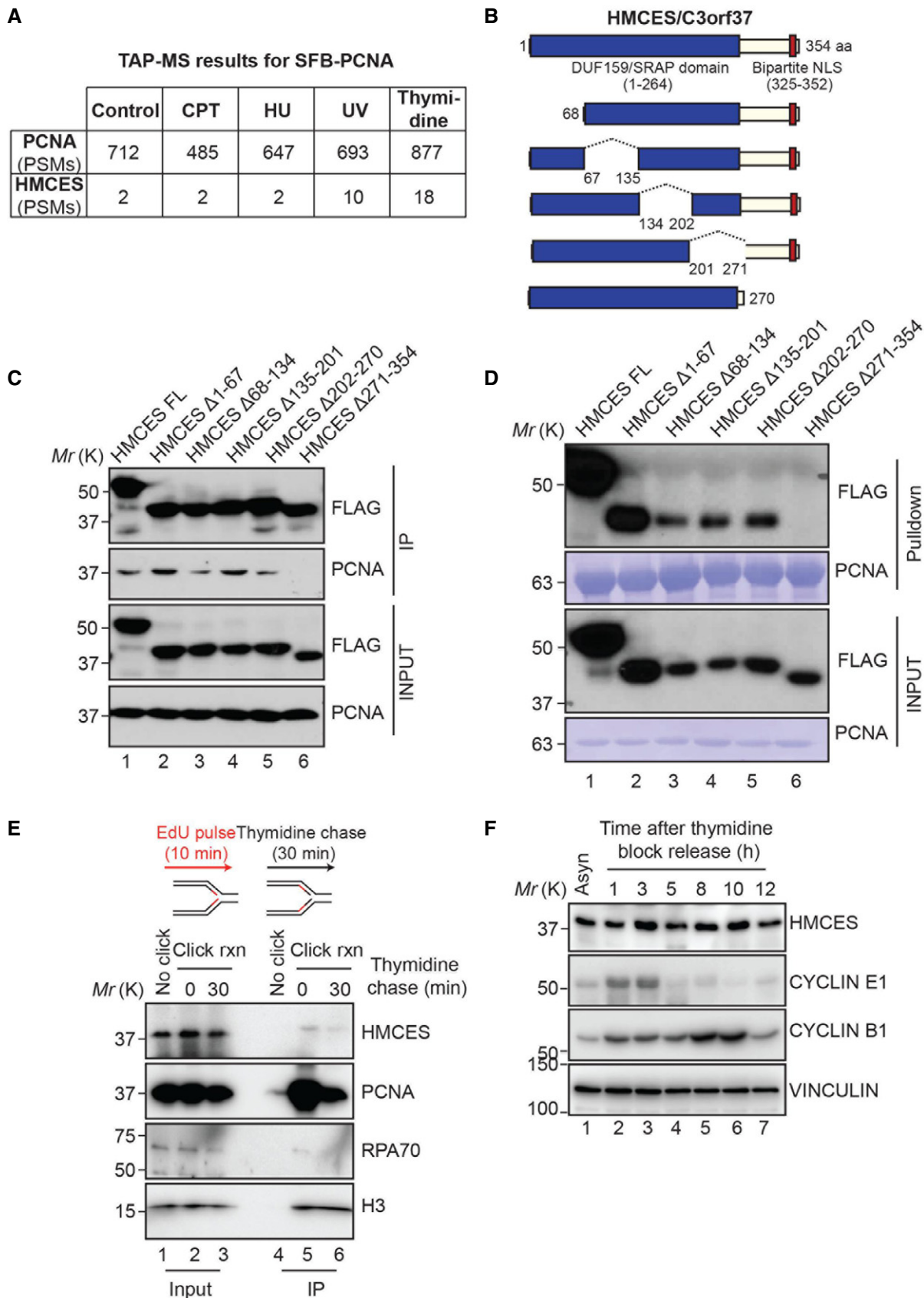


Figure 1.

levels of genomic DNA were evaluated by slot blot [20] (Fig EV4J). Our results showed no significant difference between the levels of 8-oxodG in WT and HMCES KO cells. This result is not unexpected, since in order to maintain genetic information, several glycosylases are known to act on oxidative damage pre- and post-replication and during different phases of the cell cycle (please see Fig EV3B). Many glycosylases have overlapping substrate spectra, which may explain the viability of their knockout mouse models with the exception of TDG [21]. OGG1 is a bifunctional glycosylase that can excise 8-oxodG from genome [5]. We further evaluated if treatment of OGG1 inhibitor, O8, upon H<sub>2</sub>O<sub>2</sub> exposure could potentiate the sensitivity. We did not find any significant difference in cell survival upon combination treatment in wild-type or HMCES KO cells (Fig EV4K and L). This could be due to either ineffective inhibition or presence of redundant glycosylases in cells [22]. Additionally, we explored whether HMCES could get recruited to sites of DNA damage. Although we did not observe HMCES foci formation following DNA damage, we did observe its localization to laser-induced damage sites (Fig EV4M).

### HMCES plays an important role in repair of misincorporated bases on replication fork

Both H<sub>2</sub>O<sub>2</sub> and IR generate ROS resulting in oxidized nucleotide pool and macromolecules containing oxidized bases. If inadequately sanitized, these bases upon replication can alter genomic information. Besides, HMCES has been shown to recognize epigenetic cytosine modifications in an early study [16]. Taken together, we hypothesized that HMCES could participate in the recognition and turnover of oxidized or other misincorporated bases during replication. In order to precisely evaluate the role of HMCES on replication fork, we utilized clinically used therapeutic agents such as pemetrexed (Alimta) and 5-FU [23]. Both are antimetabolites that inhibit pyrimidine biosynthesis pathway, thereby altering the pool of thymidine and resulting in increased incorporation of dUTP [12,24]. In case of 5-FU, in addition to dUTP, 5-fluoro-2'-dUTP can also be incorporated into DNA. Treatment with pemetrexed increased the levels of uracil in the genome that can be removed by glycosylases (mainly UNG) during replication, which generate AP sites as repair intermediates that can be detected (Fig EV5A).

We reasoned that using pemetrexed could help us to precisely evaluate the role of HMCES during replication, as the action of the compound is exclusively replication-dependent. Interestingly, we found that HMCES KO or knockdown cells were significantly more tolerant of pemetrexed treatment than WT cells (Figs 3A and B, and EV5B and C). Although to a lesser degree than pemetrexed, HMCES KO cells were also found to be resistant to 5-FU compared to WT cells (Fig EV5D).

Owing to their therapeutic value, correlation between BER pathway and resistance to pemetrexed and 5-FU has been widely explored. Studies have suggested that overexpression of glycosylases such as UNG and TDG can render resistance to pemetrexed and 5-FU [25,26]. We showed that pemetrexed treatment on its own does not influence expression levels of tested glycosylases (Fig EV5E). We also tested whether levels of S phase glycosylases would be altered in HMCES KO background and found no significant difference in the levels of UNG and NEIL3 glycosylases between WT and HMCES KO cells (Fig EV5F). Replication stress induces a cascade of signaling events including but not limited to phosphorylation of ATR, CHK1 and RPA [27]. Evaluation of these markers of DNA damage response revealed no defect in the activation process of replication stress response in HMCES KO cells (Fig EV5G). On the other hand, HMCES KO cells displayed higher levels of RPA phosphorylation (pS4/8-RPA2) even in untreated cells (Fig EV5G), indicating DNA damage accumulation in HMCES KO cells.

Removal of oxidized bases by glycosylases involves the generation of AP site intermediate. Hence, overexpression of glycosylases such as UNG in pemetrexed-treated cells would result in increased levels of AP sites [25]. It has been proposed that blocking or inhibiting the action of AP endonucleases can override glycosylase-mediated resistance to pemetrexed and 5-FU [28,29]. To explore whether or not resistance observed in HMCES KO cells is due to the involvement of the same BER cascade, we employed both genetic and chemical-mediated inhibition of AP endonuclease activities in WT and KO background. APEX2 interacts with PCNA through a PIP-box motif, which promotes its localization to replication fork [30]. We found that although inhibition of APEX2 in WT cells resulted in mild proliferation defect, its knockdown in HMCES KO cells did not reveal any enhanced defect (Fig 3C and D). We also utilized two chemical inhibitors of AP endonuclease (APE) activity,

**Figure 2. HMCES participates in cell proliferation and DNA damage/replication stress response.**

- A Western blotting analysis confirmed HMCES knockout in 293A cells (293A HMCES KO). Blots also included knockout cells reconstituted with WT SFB-HMCES.
- B Colony-forming capacity of HMCES KO cells was compared to that of control wild-type 293A cells.
- C Box plot showing colony-forming efficiencies of 293A wild-type control and HMCES KO cells. Box limits represent 25<sup>th</sup> and 75<sup>th</sup> percentile, centerline shows the median, and whiskers extend minimum to maximum. Data include more than three independent repeats performed in duplicates. Student's *t*-test was performed for statistical analysis (\*\*\*\**P* < 0.0001).
- D Clonogenic survival assay of 293A wild-type control and HMCES KO cells treated with various concentrations of hydroxyurea (HU) was shown. Seeding density with respect to control was indicated below each image. The images shown are representative of three biological repeats, each performed in duplicate.
- E Quantification showing survival fraction of wild-type control (WT) and HMCES KO cells upon HU treatment. Data are presented as mean ± SEM (*n* = 3, each performed in duplicates), and Student's *t*-test was performed for statistical analysis (ns, not significant; \**P* < 0.05).
- F Quantification of clonogenic survival assay upon exposure of WT and HMCES KO cells to ionizing radiation (IR). Data are presented as mean ± SEM. Quantifications are from three biological repeats performed in duplicates. Student's *t*-test was performed for statistical analysis (\**P* < 0.05; \*\**P* < 0.01).
- G, H Sensitivity assay and quantification of surviving WT control and HMCES KO cells determined by colony-forming assay upon exposure to H<sub>2</sub>O<sub>2</sub>. Experiments were repeated three independent times, each time performed in duplicates, and data are presented as mean ± SEM. Statistical significance for the corresponding experiment was analyzed by Student's *t*-test (\**P* < 0.05).
- I Bar graph showing sensitivity of WT, HMCES KO, and stably reconstituted WT cells toward H<sub>2</sub>O<sub>2</sub> treatment. Experiment was repeated two independent times with technical repeats.

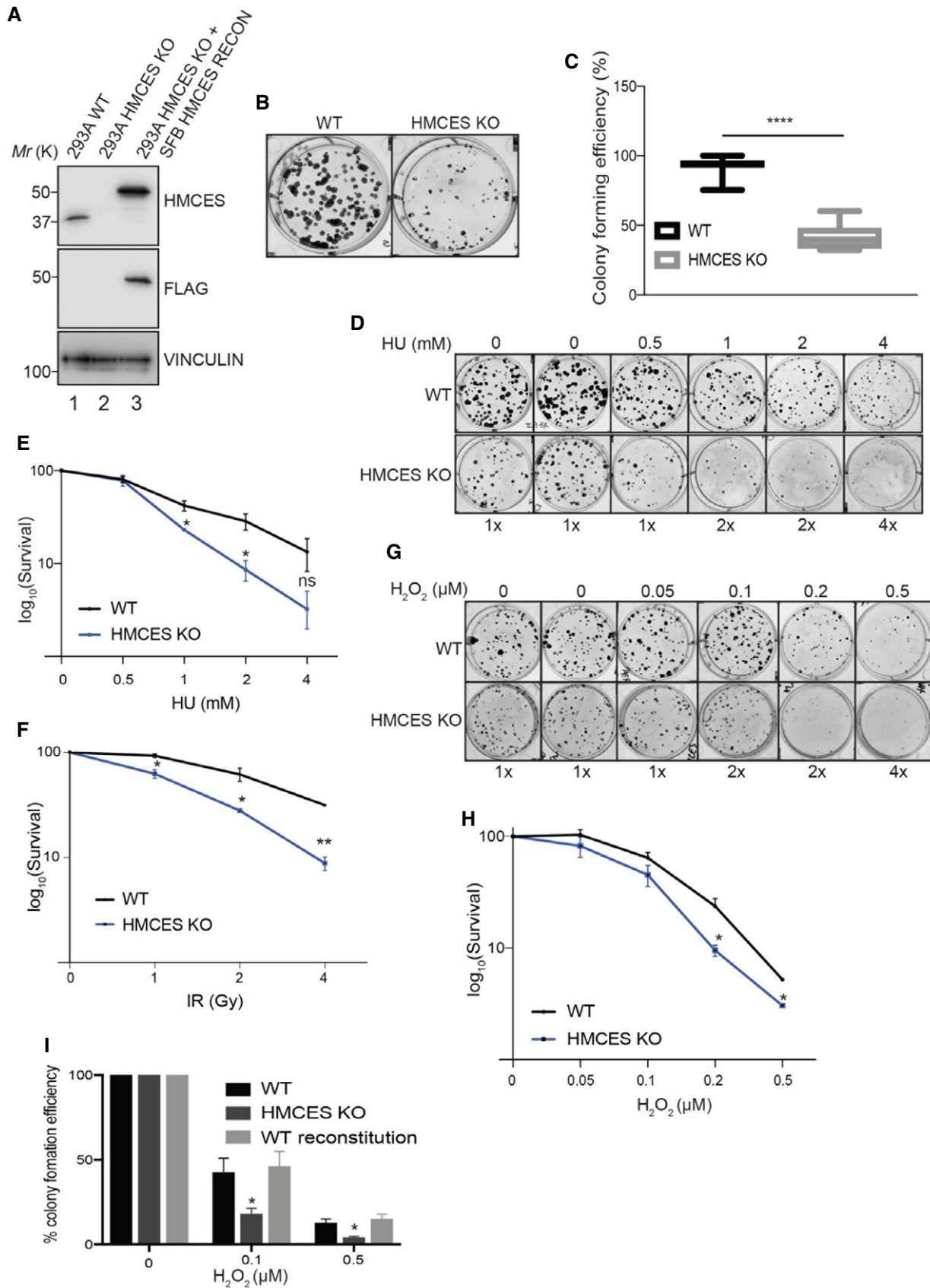


Figure 2.

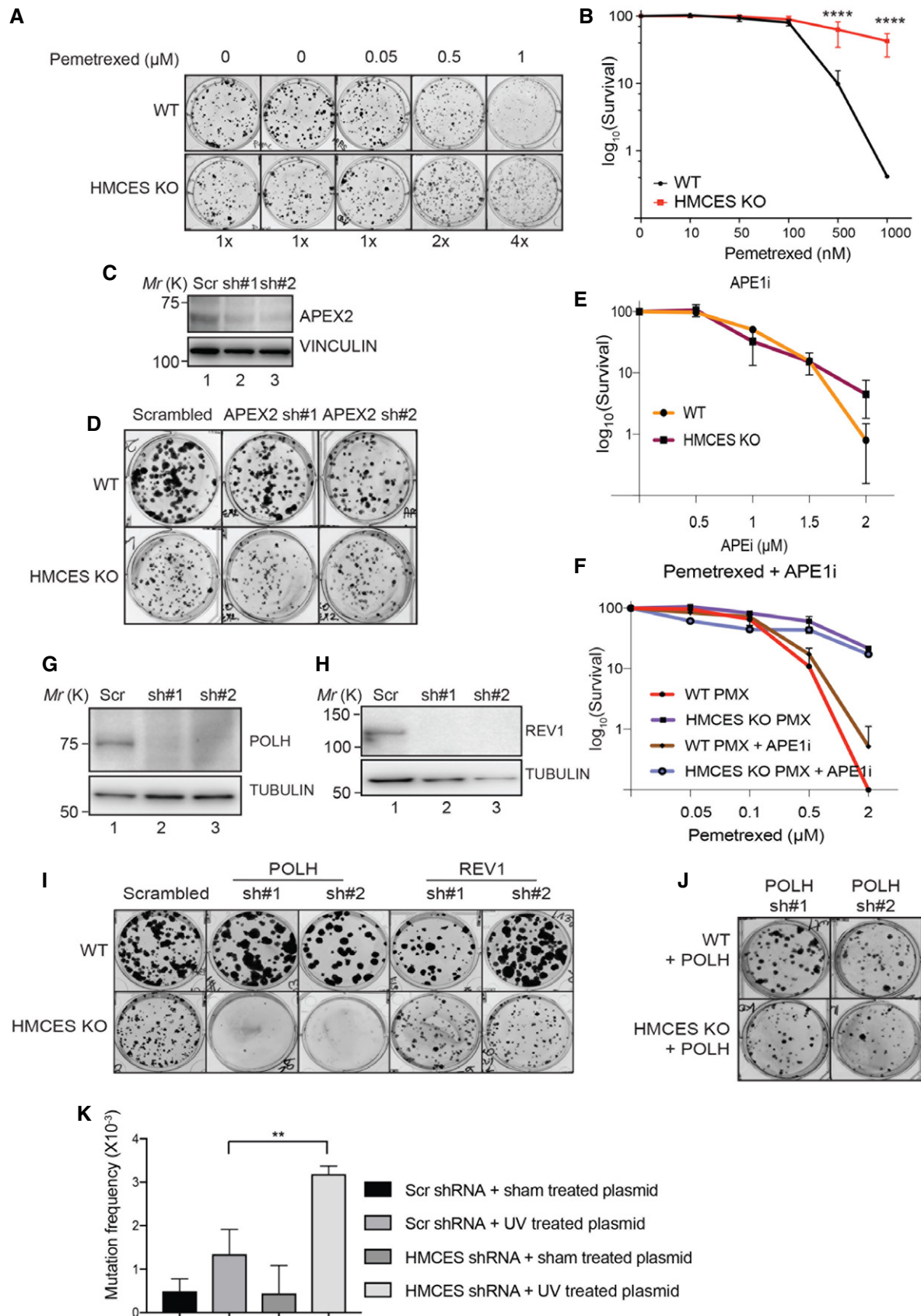


Figure 3.

**Figure 3. HMCES-mediated tolerance is imparted by the bypass of oxidative damage.**

- A, B Clonogenic assays were performed by adding increasing concentrations of pemetrexed to control wild-type (WT) 293A cells and HMCES knockout (HMCES KO) cells (A), and quantification of results was shown (B). Increasing numbers of cells were seeded with increasing concentrations of the compound to obtain optimal drug dose–response curve. Seeding density with respect to control is indicated below each image. The images shown are representative of three biological repeats, each performed in duplicate. (B) Data are presented as mean  $\pm$  SEM, and Student's *t*-test was performed for statistical analysis (\*\*\*\**P* < 0.0001).
- C Western blot showing APEX2 levels upon 293A cells infected with viruses encoding scrambled or two independent APEX2 shRNAs.
- D Colony-forming assay was performed to indicate colony-forming efficiency in 293A and HMCES KO cells upon infection with viruses encoding scrambled or APEX2 shRNAs.
- E Sensitivity assay was conducted with WT and HMCES KO cells upon treatment with AP endonuclease inhibitor III (APEi). Results are presented from two independent experiments, and data are presented as mean  $\pm$  SEM.
- F Colony-forming assay was performed with WT and HMCES KO cells upon either pemetrexed treatment alone or in combination with APEi. Data are presented as mean  $\pm$  SEM (*n* = 2 each with technical repeats).
- G, H Western blotting revealed levels of POLH (G) and REV1 (H) in two independent clones upon selection following transfection with indicated shRNA.
- I Colony-forming assay was conducted to reveal proliferation of WT, POLH KD, REV1 KD, HMCES KO, HMCES KO + POLH KD, and HMCES KO + REV1 KD cells.
- J Representative images showing proliferation of respective shRNA-resistant reconstitution of POLH in 293A and HMCES KO cells stably expressing POLH shRNA. Experiment was repeated two independent times in duplicates.
- K Mutagenesis frequency analysis was conducted in 293T scrambled and 293T HMCES shRNA cells using supF shuttle vector-based assay system. Experiments were repeated three independent times, and data are presented as mean  $\pm$  SEM. Student's *t*-test was used to calculate statistical significance (\*\**P* < 0.01).

methoxyamine (MX), and APE1 inhibitor III (APEi). MX structurally modifies AP site by covalently crosslinking to open-chain aldehyde group of AP site, thereby obstructing AP endonucleases, whereas APEi targets active site of both APEX1 and APEX2 [31,32]. Upon co-treatment of pemetrexed and MX in WT cells, only modest increase in sensitivity was observed in WT cells in dose-dependent manner (Fig EV5H). This is in accordance with reported results with pemetrexed-sensitive cells [28]. However, interestingly, contrary to UNG-overexpressing pemetrexed-resistant cells, which lose their survival benefit upon MX treatment, HMCES KO cells still remain unresponsive (Fig EV5I). These data suggest that resolution of misincorporated bases or intermediate AP sites generated in HMCES KO cells is being carried out by an alternative repair pathway. In agreement, treatment with APEi also fails to sensitize HMCES KO cells to pemetrexed treatment (Fig 3E and F).

In addition to BER pathway, translesion bypass can be employed to replicate through these lesions. In the case of persisting oxidative damage on ongoing replication fork, error-prone bypass mechanisms may take over, which could result in completion of replication, although probably at the cost of compromised genetic integrity. We explored whether knockdown of TLS polymerases POLH or REV1 would affect viability of HMCES KO cells (Fig 3G–I). We found that knockdown of TLS polymerase REV1 in HMCES KO mildly decreased colony-forming efficiency of both WT and HMCES KO cells. However, colony-forming assay showed a drastic reduction in the proliferation of HMCES KO cells upon POLH knockdown (Fig 3I). Reconstitution with shRNA-resistant POLH prior to POLH knockdown can rescue this phenotype (Figs 3J and EV5J). Further, we observed increased chromatin enrichment of TLS polymerases, POLH and REV1, in HMCES KO compared to those in WT cells (Fig EV5L and M). Further, we employed Sup F mutation assay system to examine the effects of HMCES deficiency on UV damage-induced mutagenesis. Mutation frequency in HMCES KO increased significantly following DNA damage as compared to that in WT cells (Fig 3K). Thus, our results indicate that cells deficient in HMCES may rely more on TLS polymerases, and therefore, it is possible that pemetrexed resistance observed in HMCES-deficient cells may be overcome by inhibition of TLS pathway. To test this possibility, we utilized pooled scrambled, POLH, and REV1 shRNA-infected WT and HMCES KO cells. Interestingly, we found that knockdown of

POLH, but not REV1, in HMCES KO cells made these cells sensitive to pemetrexed treatment (Fig EV5O and P). Taken together, our results suggest that HMCES and BER machinery may act in the same genetic pathway and HMCES deficiency renders cells dependent on TLS pathway for survival under oxidative damage.

#### Loss of homologous recombination repair (HRR) factors are synthetic lethal with HMCES deficiency

Next, we sought to systematically identify DNA repair factors that can act in synergistic or antagonistic manner with HMCES. To do this, we performed CRISPR-CAS9 screen with a small DDR (DNA damage response) sgRNA library on WT and HMCES KO cells. We used MAGeCK and BAGEL data analysis tools to calculate *P*-value and FDR for each gene and focused on the genes that selectively affect survival fitness in HMCES KO cells (Figs 4A and B, and EV6A, Dataset EV1). Pathway analysis performed using the top 50 genes responsible for negative selection showed enrichment for Fanconi anemia and HRR pathways (Fig EV6B). HRR factors, such as CtIP, PALB2, BRCA1, and BRCA2, were the strong HMCES synthetic lethal hits in this screen. As each gene in our library is targeted by 10 individual sgRNAs, we further analyzed how many sgRNAs responsible for our top candidates showed significant changes in our screen. We found that 10/10 CtIP sgRNAs were downregulated in HMCES KO cells (Fig 4C), indicating a strong synthetic lethal interaction. Additionally, other HRR factors, such as BRCA1 (9/10), PALB2 (8/10), and BRCA2 (7/10), also displayed synthetic lethality with HMCES (Fig 4C). Next, we analyzed whether homologous recombination repair would be defective in HMCES KO cells by examining RAD51 foci formation and resolution after irradiation. While HMCES KO cells showed slightly fewer RAD51 foci after irradiation, which could be attributed to their proliferation defect, resolution of RAD51 foci was not hindered in HMCES KO cells (Fig EV6C and D), suggesting functioning HRR pathway in the absence of HMCES. We further validated the synthetic interaction between HMCES and HRR factors by knockdown of HRR factors, such as CtIP and BRCA2, in HMCES-deficient cells (Fig 4D and E). Consistent with our screen results, knockdown of either CtIP or BRCA2 adversely affected cell growth, which decreased further when combined with HMCES KO (Fig 4F and G).

The conservation of HMCES through lower eukaryotes and prokaryotes predates development of epigenetic regulation, which suggests a conserved and fundamental role of HMCES in these organisms. In bacteria, the SOS response is a regulatory network

that is activated upon genotoxic stress and helps environmental adaptation of the organism. Its interaction with PCNA and presence on the replication fork equips it to act as a proofreader to ensure genome integrity during replication. How oxidative base damage on

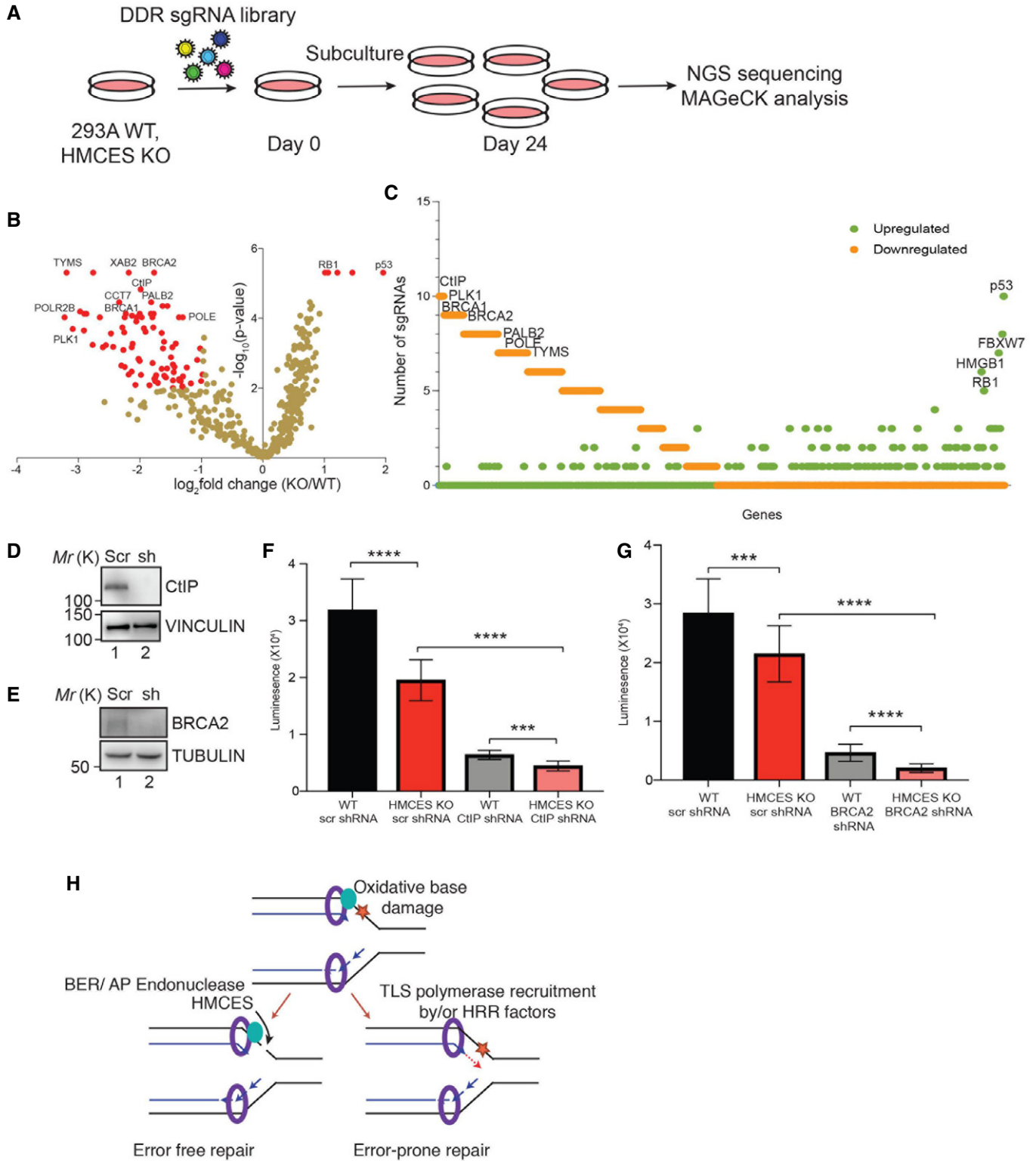


Figure 4.



**Figure 4. CRISPR-CAS9-based synthetic lethality screen conducted in HMCES KO cells reveals genetic interaction between HMCES and homologous recombination pathway.**

- A Schematic representation of DDR CRISPR-CAS9 screen performed in WT and HMCES KO cells.
- B Volcano plot showing DDR CRISPR-CAS9 screen for HMCES KO cells.  $-\log_{10}(P\text{-value})$  is plotted against  $\log_2(\text{HMCES KO/WT})$  fold change. Genes showing significant positive and negative enrichment are colored in red, and top enriched candidates are also labeled.
- C Plot showing number of sgRNAs that are negatively or positively enriched for each gene in DDR library.
- D, E Western blots showing levels of CtIP (D) and BRCA2 (E) upon shRNA-mediated knockdown in 293A cells.
- F, G Cell proliferation measured using CellTiter-Glo assay in 293A and HMCES KO cells without or with transfection with viruses encoding CtIP (F) and BRCA2 (G) shRNAs. Each experiment was repeated three independent times done in triplicates each time. Data were represented as mean  $\pm$  SEM. Student's *t*-test was used to calculate statistical significance (\*\*\**P* < 0.001; \*\*\*\**P* < 0.0001).
- H Our current working model depicting HMCES mechanism of action on replication fork. Upon encountering oxidative base damage on replication fork, HMCES along with BER machinery can successfully remove modified base to resume replication. This mechanism would result in error-free replication and maintain genomic integrity between parental and nascent replication forks. In the absence of HMCES, however, the replication fork can proceed only by replicating through the damage, often by misrecognition and misincorporation of bases by replicative or translesion polymerases, leading to replication errors. HRR factors such as CtIP, BRCA2, BRCA1, and PALB2 are indispensable for processing the damage, possible recruitment of TLS polymerase, and replication fork restart.

the replication fork gets repaired in an error-free manner is not well characterized. Based on our results, we hypothesized that HMCES on the replication fork drive them toward error-free resolution (Fig 4H). We found that inhibition of AP endonucleases does not exacerbate cell death in HMCES KO cells, suggesting AP endonucleases may act in concurrence with HMCES for the resolution of AP sites. In the absence of HMCES, however, error-prone bypass mechanisms may take over, which could result in remarkably greater cell survival, although probably at the cost of compromised genetic integrity. Knockdown of TLS polymerases, especially polymerase eta (POLH), significantly reduces viability of HMCES KO cells, demonstrating that HMCES-deficient cells may rely on TLS pathway for survival.

Recently, Cortez and colleagues reported that HMCES-SRAP domain is responsible for shielding AP sites achieved by covalently crosslinking to AP sites to form DNA-protein crosslinks [14]. AP sites are chemically unstable and present in equilibrium with ring-closed cyclic hemiacetals and open-chain aldehyde forms [33]. Open-chain aldehyde forms are highly reactive and thus form the basis for various molecular biology tools such as ARP probe and methoxyamine (MX) [31,32]. Along with KU and human ribosomal protein S3, nucleoside diphosphate kinase, PARP-1, histones H3, H4, many metabolic proteins have been shown to react with AP sites [34–40]. Similarly, most of the glycosylases tend to remain bound to their resulting products and even possess a higher affinity toward AP sites than their actual substrates, and therefore, their release from AP sites is considered as a rate-limiting step in BER [21,41–45]. It is suggested that post-translational modifications such as phosphorylation and ubiquitination of glycosylases may be important for regulating the rigid binding of glycosylases to AP sites [46]. Our study suggests that HMCES and AP endonucleases may act in the same branch of repair pathway and HMCES deficiency results in utilization of alternate error-prone repair of DNA lesions. This raises the possibility that HMCES may act in synergy with AP endonucleases upon the generation of AP site intermediate. It may protect exposed AP sites until AP endonucleases are recruited. Alternatively, HMCES may also trigger the turnover of AP site-endonuclease complexes and promote the release of AP endonucleases. Precisely how HMCES protects AP sites and funnels such lesions to error-free repair needs to be further elucidated.

While this manuscript was under revision, a more recent study reported that HMCES could also enable microhomology-mediated end joining during class-switch recombination (CSR) through its

DNA binding activities [47]. We would like to point out that during antibody diversification process, activation induced deaminase (AID) introduces targeted uracils specifically at immunoglobulin loci, which initiates base lesions for both somatic hypermutation and CSR. It has been shown that knockout of UDG results in disturbed antibody diversity [48,49]. It would be of interest to explore whether HMCES acts in this pathway along with microhomology-mediated repair.

Our results demonstrated that HMCES is important for replication stress response and cell survival. As ROS can generate more than 100 different types of base oxidative damages, it would be interesting to evaluate the breadth and the range of HMCES action, especially on other common types of DNA lesions such as fapy-G, 8-oxodA, and others. There may be additional regulation and function of HMCES at replication fork. An early study evaluating interaction of human host proteins with dengue viral particles suggests that HMCES is a candidate regulator of early replication of viral particles [50]. In addition, a system-wide MS study reported the possibility of HMCES sumoylation following HU treatment [51], which needs to be verified and its significance further investigated. Additionally, we propose that HMCES level may be used as a predictor of pemetrexed response in cells, which warrants further validation. Moreover, we speculate that in the absence of HMCES, cells are able to bypass the modified bases during replication and hence are tolerant of these modified bases. However, this error-prone bypass may come at the cost of compromised genomic integrity. TLS polymerases especially POLH have been shown to be responsible for cell cycle checkpoint evasion and increased survival after replication stress and/or treatment with genotoxic agents [52,53]. POLH has also been correlated with tolerant response of isogenic NER-defective cell lines to cisplatin [54].

In this study, we also performed CRISPR-CAS9 screen utilizing a DDR sgRNA library and revealed strong synthetic lethality of HMCES with homologous recombination pathway. CtIP, BRCA2, BRCA1, and PALB2 were among the top candidates in this screen. Interestingly, synthetic lethality between APEX2 and BRCA2 was reported recently [55]. Although the exact mechanism underlying this synthetic lethality interaction remains unknown, it was suggested that BRCA2-mutant cells may depend on BER pathway for survival. Besides their conventional roles in homologous recombination by facilitating strand invasion, BRCA2 and PALB2 have also been shown to be crucial for recruitment of POLH at stalled replication fork and restart of DNA synthesis [56]. Further, TLS polymerases have been shown to be important for DNA synthesis at D-

loop recombination intermediates [57,58]. It will be interesting to further explore whether the observed synthetic lethality between HMCES or APE2 and HRR components is due to failed replication restart and/or due to hindered lesion bypass pathway.

## Materials and Methods

### Cell lines, transfection, and generation of stable cell lines

293T and 293A cells were procured from ATCC and grown with Dulbecco's modified Eagle's medium (DMEM) containing 10% fetal calf serum (FCS) in 37°C with 5% CO<sub>2</sub>. A549, Calu-1, H322, H358, H460, H1299, and H1975 cells were gifts from Dr. Khandan Keyomarsi. All plasmid transfections were performed using polyethylenimine (PEI). In brief, cells were seeded a day before transfection. For transfection, both 9 µg of PEI and 2 µg of plasmid were diluted in PEI, separately. Diluted PEI was added to the plasmid solution, followed by incubation at room temperature for 15 min, and the mixture was added to cells. The transfection reaction was scaled up or down as needed. For the generation of stable cell lines, transfected 293T cells were diluted, seeded, and selected with puromycin (Sigma Aldrich#P8833). Individual clones were picked and analyzed by Western blotting. Generation of stable cells for complementation experiments in KO cells was also performed similarly.

### Plasmids

pCMV-SPORT6 vector-containing HMCES CDS was purchased from Dharmacon (Cat No. MHS6278-202759729). CDS was amplified and cloned in to pDONR201 and pDEST-SFB vectors. All the mutations and deletions were made in pDONR201-HMCES vector and transferred to pDEST-SFB for mammalian expression studies. PCNA was cloned in pDEST17 (Thermo Fisher#11803012) for bacterial expression. sgRNAs were cloned in LentiCRISPRV2 (addgene#52961) for the generation of knockout cell lines. pMD2.G (#12259) and psPAX2 (#12260) vectors were procured from addgene. pGIPZ-based shRNAs for scrambled, POLH (#RHS4430-200242604; RHS4430-200170042), REV1 (#RHS4430-200191677; RHS4430-200232148), HMCES (#RHS4430-200222506), APEX2 (#RHS4430-200242835; RHS4430-200244959), CtIP (#RHS4430-200160039), and BRCA2 (#RHS4430-200253065) were obtained from MD Anderson shRNA and ORFome core facility (Horizon discovery Dharmacon). For POLH reconstitution assays, silent mutations were introduced in POLH CDS individually in each POLH shRNA seed sequence and cloned in pDEST-mCherry.

### shRNA knockdown and reconstitution

pGIPZ-based vectors were used for the generation of stably expressing shRNA. Briefly, constructs encoding scrambled and gene-specific shRNAs were transfected into 293A or HMCES KO cells. 24 h post-transfection, cells were sorted to retrieve brightest GFP<sup>+</sup> cells. These cells were expanded further in puromycin-containing medium. For generation of POLH reconstitution cells, 293A and HMCES KO cells were first transfected with pDEST-mCherry POLH vector and selected with G418, followed by infection with POLH shRNA and selection with puromycin. Highest expressing mCherry and GFP<sup>+</sup> cells were

collected by flow cytometry. For sensitivity assay with pemetrexed for POLH and REV1 shRNA, 293A and HMCES cells were infected with respective lentivirus and used for assays without sorting.

### Mass spectrometry

HEK239T cells containing stable SFB-tagged PCNA were used for MS analysis under different DNA-damaging conditions as described previously [1].

### Immunoprecipitation and GST pull-down

For immunoprecipitation experiments, cells were lysed in 1XNETN buffer on ice for 30 min. Lysates were clarified by centrifugation at 17,949 g for 10 min. 2% input samples were removed at this point, and buffer-equilibrated streptavidin beads (GE Healthcare # 17511301) were added to all samples and incubated for 2 h in 4°C on rotation. Beads were washed with 1XNETN buffer thrice and bound proteins were eluted by boiling beads in 2× Laemmli buffer and loaded on to the SDS-PAGE. Western blot was performed using specified antibodies. For GST pull-down experiments, GST-PCNA was added instead of streptavidin beads and the rest of the steps were performed as described above.

### Western Blotting analysis

Standard protocols for sodium dodecyl sulfate-polyacrylamide gel electrophoresis (SDS-PAGE) and immunoblotting were followed [59]. PVDF membrane (Millipore) was used to transfer proteins from polyacrylamide gels and visualized by Bio-Rad Chemidoc imaging system. Antibodies used in the study are following FLAG (Sigma-Aldrich # F3165), PCNA (Cell Signaling Technology # 2586), HMCES (Protein Atlas # HPA044968), VINCULIN (Sigma-Aldrich#V9131), UNG (Santa Cruz # sc-390255), NEIL3 (Santa Cruz # sc-393703), TDG (Santa Cruz # sc-376652), CYCLIN A (Santa Cruz # sc-271682), CYCLIN B1 (Santa Cruz # sc-7393), CYCLIN E (Santa Cruz #sc-377100), RPA70 (EMD Millipore#NA13), RAD51 (Cell Signaling Technology # 8875), pATR (GeneTeX#GTX128145), pChk1 (Cell Signaling Technology 2341), pRPA (Bethyl Laboratory# A300-245A), CtIP (Cell Signaling Technology #9201), APEX2 (Thermo Scientific # PA5-72607), BRCA2 (Novus Biologicals #MAB2476), 8-oxodG (JaiCA, clone#N45.1), REV1 (Thermo Scientific # PA5-46793), and POLH (Cell Signaling Technology #13848).

### Cell fractionation

Cells were treated with indicated concentrations of pemetrexed and 5-FU for 24 h. Cells were collected and lysed in 1XNETN buffer-containing protease inhibitors. After high speed centrifugation (17,949 g for 30 min), soluble fraction was immediately transferred into fresh tube. Chromatin fraction was washed twice in 1× NETN with 10 min each time. Further, chromatin was digested with Turbonuclease (Accelagen # N0103) in nuclease buffer (10 mM Tris-Cl, pH 8.0, 1 mM MgCl<sub>2</sub>) in the presence of protease inhibitors. After 15-min incubation at 37°C, lysate was spin down and supernatant was collected. Protein concentrations of soluble and digested chromatin were estimated by nanodrop, equalized and boiled in 2× laemmli's buffer, and used for Western blot analysis.

### aniPOND analysis

Recruitment of HMCES on replication fork was performed by aniPOND (accelerated native iPOND) as described earlier [60]. Briefly, cells were labeled with thymidine analog 5-ethynyl-2'-deoxyuridine (EdU) (Sigma-Aldrich# 900584) for 10 min, thymidine chase was performed for 30 min if required, and otherwise, cells were scraped in nuclear extraction buffer (NEB) [60]. Click reaction was performed for 1 h, nucleus was sonicated, and proteins were captured using streptavidin beads by overnight incubation at 4°C. Beads were washed three times, elution of replication fork-associated proteins was done by heating beads at 95°C for 10 min, and complex was analyzed by Western blotting with specific antibodies.

### CRISPR-CAS9-mediated generation of knockout cells and reconstitutions

Knockout cells were generated as described earlier [1]. Briefly, cells were transfected with LentiCRISPRv2 plasmid-containing sgRNA. After 24 h, cells were seeded in 96 wells (1 cell/well). Clones were allowed to grow and confirmed by Western blotting and sequencing. Sequences of sgRNAs used for generating knockout cells are provided below:

HMCES sgRNA 1: 5' CACCGTGCCTACCAGGATCGGCG 3'  
HMCES sgRNA 2: 5' CACCGCCAGCAGCGGCTCCCGAG 3'

For the generation of reconstituted cells, constructs encoding WT and mutant HMCES were transfected into 293A HMCES KO cells. After 24 h, 20 cells (1 cell/well) were seeded in 96-well plate. Clones are transferred to 48-well plate after sufficient growth and confirmed by Western blotting. Clones with undetectable levels of HMCES at protein levels were further confirmed by sequencing. Briefly, genomic DNA was isolated, amplified, cloned in T-vector (promega), and sequenced (Eurofin genomics).

### Cell survival assay

Cells were counted and seeded with either equal or increasing number (250, 500, or 1,000) with increasing concentrations of drug, as indicated. For Hydroxyurea (Sigma-Aldrich#H8627), indicated concentrations of compounds were added for 24 h and cells were washed and replenished with fresh medium. Cells were allowed to grow for 10 days, and colonies were visualized with crystal violet solution (Sigma-Aldrich#HT90132). For pemetrexed (Sigma-Aldrich#CDS024404), methoxyamine (Sigma-Aldrich#226904), O8 (Millipore Sigma# SML1697), and APE1 III (Millipore Sigma# 262017) inhibitor cells were treated with indicated concentrations and compounds were left through the entire duration of colony-formation. For colony-forming assay with H<sub>2</sub>O<sub>2</sub> (Sigma-Aldrich#216763), cells were treated with indicated concentrations for 30 min, washed, and allowed to grow for 10 days before staining with crystal violet. All colony-forming assays were performed in duplicates and repeated three independent times unless indicated otherwise. Colonies were scored manually and plotted with GraphPad Prism, and images were collected using Bio-Rad Chemidoc imaging system.

### Luminescent cell viability assay

Cell viability experiments with CtIP and BRCA2 shRNA-mediated knockdown in 293A and HMCES KO cells were done using Cell-Titer-Glo (Promega#G7570). 293A and HMCES KO cells with scrambled shRNA were used as control. Briefly, 100 cells were seeded in 96 wells in triplicates. After 48 h, cells were treated as manufacturer's instructions and luminescence was recorded. Each experiment was performed for minimum of three times.

### Cell cycle analysis

For the analysis of expression of various proteins in different cell cycle phases, cells were seeded in a 6-well plate and were then synchronized at G1/S boundary with double thymidine block [61]. Cells were released into fresh medium and collected at indicated time points, half of the samples were used to cell cycle analysis, and rest boiled in 2× Laemmli buffer and analyzed by Western blotting. For cell cycle analysis, cells were collected and fixed in 70% ethanol, washed, and incubated with 1XPBS-containing propidium iodide (50 µg/ml) and RNase A (50 µg/ml) for 30 min at 37°C. Samples were analyzed on Gallios Flow Cytometer. Data were analyzed and plotted with the help of FlowJo software.

### Detection of apoptosis

293A and HMCES KO cells were treated with H<sub>2</sub>O<sub>2</sub> (200 µM) for 15 min, washed, and allowed to recover for 24 h. Cells were collected including the floating cells, if any and stained with Annexin V-FITC and PI according to manufacturer's instructions (BD Biosciences # 556547). Samples were analyzed on Gallios Flow Cytometer, analyzed, and plotted.

### Mutation frequency

293T cells infected with scrambled or HMCES shRNA were used for the assay. Shuttle vector pMY189 was kind gift from Prof Tomonari Matsuda (Koyoto University, Japan) and Prof Haruhiko Sugimura (Hamamatsu University School of Medicine, Japan). SupF tRNA-containing shuttle vector, pMY189, was UV irradiated (500 J/m<sup>2</sup>). Untreated and UV-irradiated (2 µg) plasmid was transfected into the cells. 48 h post-transfection, plasmid was retrieved by alkaline lysis method. In order to remove unreplicated vector, plasmids were digested with Dpn I. Plasmid was then transformed into MBM7070 *E. coli* competent cells and plated in the presence of Ampicillin (100 µg/ml) and IPTG/X-GAL (1 mM/100 µg/ml). A total number of colonies (blue and white) were counted, and white colonies in each case were considered mutant colonies. Experiment was repeated three independent times. Mutation frequency was determined by enumerating the ratios between mutant and wild-type colonies.

### Immunofluorescence staining

293T cells containing stable expression of SFB-HMCES were seeded on glass bottom dish a day before microirradiation. Microirradiation was performed using 365 nm UV laser Micropoint system supported with Nikon TE200 Fluorescence microscope. Cells were fixed in 3% paraformaldehyde (10 min) followed by permeabilization by

incubation with 0.5% Triton X-100 for 5 min at RT. Cells were washed and incubated with FLAG (1:1,000) and  $\gamma$ H2AX (1:500) in 3% BSA containing 1XPBST for 1 h at 37°C. For RAD51 foci quantification, cells were treated with IR (2 Gy), fixed, and permeabilized as described above. Cells were washed and incubated with secondary antibodies (1:1,000) conjugated with FITC and Rhodamine and mounted with DABCO antifade. Cells were visualized by a Nikon Fluorescence microscope.

### Quantification of AP sites and 8-oxodG

Cells were treated with pemetrexed as indicated, and cells were collected at indicated time points. DNA was isolated using Qiagen genomic DNA isolation kit for AP site quantification and quantified using Nanodrop. 1  $\mu$ g of DNA was incubated with 1 mM ARP-probe for 30 min at room temp followed by ethanol precipitation. Pellet was washed minimum of three times to remove unbound ARP-probe. DNA was solubilized in TE (10:1) and quantified again. DNA was heated at 95°C for 10 min and snap cooled on ice, and equal volume of chilled 2M ammonium acetate was added before blotting using slot blot system to Hybond-N+ membrane (Amersham). After slot blot, membrane was dried and UV crosslinked. Methylene blue was used to stain membrane after antibody incubation and developed to visualize the loading of DNA. For quantification of 8-oxodG, cells were treated with KBrO<sub>3</sub> (20 mM) for 1 h. Cells were allowed to recover and collected at indicated time points. Genomic DNA was isolated and quantified, and 500 ng of genomic DNA was used for slot blot as described above and incubated with 8-oxodG antibody after UV crosslinking.

### CRISPR-CAS9 DDR screen

We designed CRISPR DNA damage sub-library containing 4530 sgRNAs, targeting 365 genes with either a known or suspected DNA damage response or repair function [62], together with 45 core-essential genes and 50 non-essential genes. If possible, 10 sgRNAs were designed for each gene. The DDR sub-library was cloned into lentiCRISPRv2 plasmid (Addgene). 293A or 293A/HMCES knockout cells were transduced with CRISPR DDR sub-library lentivirus at MOI of ~0.3. After puromycin selection for 3 days, cells were collected as the initial time point T0. To identify HMCES synthetic lethal genes, cells were passaged every 3 days for 24 days and maintained at 1,000-fold coverage.

Five million cells (1,000-fold coverage) were harvested at T0 and T24 for genomic DNA extraction using QIAamp DNA Blood Midi Kit (Qiagen). sgRNA inserts were amplified by PCR using NEBNext<sup>®</sup> Q5<sup>®</sup> Hot Start HiFi PCR Master Mix (New England Biolabs). Illumina TruSeq adapters with i5 and i7 barcodes were added in a second round of PCR, and PCR products were sequenced on an Illumina NextSeq 500 High Output platform to determine sgRNA representations in each sample. NGS sequencing reads were aligned to the DDR sub-library, and each sgRNA was counted using MAGECK [63]. The sgRNA reads were processed with MAGECK and BAGEL [64].

### Statistical analysis

Statistical significance was determined by using GraphPad Prism software. Data sets are shown as mean  $\pm$  SEM. For comparison

between two groups, unpaired Student's *t*-test was used. Number of independent experiments and number of repeats in each experiment are described in figure legends. *P*-values are two-tailed, and results were considered significant with  $P < 0.05$  (\* $P < 0.05$ ; \*\* $P < 0.01$ ; \*\*\* $P < 0.001$ ; \*\*\*\* $P < 0.0001$ ).

## Data availability

The mass spectrometry proteomics data have been deposited to the ProteomeXchange Consortium via the PRIDE partner repository. The accession number for the MS data reported in this paper is PRIDE: PXD011727, and URL has been provided below: <https://www.ebi.ac.uk/pride/archive/projects/PXD011727>.

**Expanded View** for this article is available online.

### Acknowledgements

We thank all the members of the Chen laboratory for their help and constructive discussions. This work was supported in part grants from the Cancer Prevention & Research Institute of Texas (RP160667) and the U.S. National Institutes of Health (CA157448, CA193124) to J.C. J.C. also received support from the Pamela and Wayne Garrison Distinguished Chair in Cancer Research. We thank MD Anderson's Flow Cytometry and Cellular Imaging Facility (supported by MD Anderson's NIH Cancer Center Support Grant, P30CA016672) for their help with the flow cytometry experiments. Dr. Mrinal Srivastava received support from an MD Anderson Odyssey postdoctoral fellowship.

### Author contributions

MS and JC conceived the project and designed the experiments. MS, DS, HZ, ZC, MT, and LN performed the experiments. MS and JC wrote the manuscript with input from all authors.

### Conflict of interest

The authors declare that they have no conflict of interest.

## References

1. Srivastava M, Chen Z, Zhang H, Tang M, Wang C, Jung SY, Chen J (2018) Replisome dynamics and their functional relevance upon DNA damage through the PCNA interactome. *Cell Rep* 25: 3869–3883 e3864
2. Moldovan GL, Pfander B, Jentsch S (2007) PCNA, the maestro of the replication fork. *Cell* 129: 665–679
3. Mailand N, Gibbs-Seymour I, Bekker-Jensen S (2013) Regulation of PCNA-protein interactions for genome stability. *Nat Rev Mol Cell Biol* 14: 269–282
4. Maynard S, Schurman SH, Harboe C, de Souza-Pinto NC, Bohr VA (2009) Base excision repair of oxidative DNA damage and association with cancer and aging. *Carcinogenesis* 30: 2–10
5. van Loon B, Markkanen E, Hubscher U (2010) Oxygen as a friend and enemy: how to combat the mutational potential of 8-oxo-guanine. *DNA Repair* 9: 604–616
6. McCullough AK, Dodson ML, Lloyd RS (1999) Initiation of base excision repair: glycosylase mechanisms and structures. *Annu Rev Biochem* 68: 255–285
7. Markkanen E, Castrec B, Villani G, Hubscher U (2012) A switch between DNA polymerases delta and lambda promotes error-free bypass of 8-oxo-G lesions. *Proc Natl Acad Sci USA* 109: 20401–20406

8. Shibutani S, Takeshita M, Grollman AP (1991) Insertion of specific bases during DNA synthesis past the oxidation-damaged base 8-oxodG. *Nature* 349: 431–434
9. Yoon JH, Bhatia G, Prakash S, Prakash L (2010) Error-free replicative bypass of thymine glycol by the combined action of DNA polymerases kappa and zeta in human cells. *Proc Natl Acad Sci USA* 107: 14116–14121
10. Avkin S, Adar S, Blander G, Livneh Z (2002) Quantitative measurement of translesion replication in human cells: evidence for bypass of abasic sites by a replicative DNA polymerase. *Proc Natl Acad Sci USA* 99: 3764–3769
11. Hanauske AR, Chen V, Paoletti P, Niyikiza C (2001) Pemetrexed disodium: a novel antifolate clinically active against multiple solid tumors. *Oncologist* 6: 363–373
12. Longley DB, Harkin DP, Johnston PG (2003) 5-Fluorouracil: mechanisms of action and clinical strategies. *Nat Rev Cancer* 3: 330–338
13. Markkanen E (2017) Not breathing is not an option: how to deal with oxidative DNA damage. *DNA Repair* 59: 82–105
14. Mohni KN, Wessel SR, Zhao R, Wojciechowski AC, Luzwick JW, Layden H, Eichman BF, Thompson PS, Mehta KPM, Cortez D (2019) HMCES maintains genome integrity by shielding abasic sites in single-strand DNA. *Cell* 176: 144–153 e113
15. Aravind L, Anand S, Iyer LM (2013) Novel autoproteolytic and DNA-damage sensing components in the bacterial SOS response and oxidized methylcytosine-induced eukaryotic DNA demethylation systems. *Biol Direct* 8: 20
16. Spruijt CG, Gnerlich F, Smits AH, Pfaffeneder T, Jansen PW, Bauer C, Munzel M, Wagner M, Muller M, Khan F et al (2013) Dynamic readers for 5-(hydroxy)methylcytosine and its oxidized derivatives. *Cell* 152: 1146–1159
17. Baharoglu Z, Mazel D (2014) SOS, the formidable strategy of bacteria against aggressions. *FEMS Microbiol Rev* 38: 1126–1145
18. Kweon SM, Zhu B, Chen Y, Aravind L, Xu SY, Feldman DE (2017) Erasure of tet-oxidized 5-methylcytosine by a SRAP nuclease. *Cell Rep* 21: 482–494
19. Tsutakawa SE, Lafrance-Vanasse J, Tainer JA (2014) The cutting edges in DNA repair, licensing, and fidelity: DNA and RNA repair nucleases sculpt DNA to measure twice, cut once. *DNA Repair* 19: 95–107
20. Ballmaier D, Epe B (1995) Oxidative DNA damage induced by potassium bromate under cell-free conditions and in mammalian cells. *Carcinogenesis* 16: 335–342
21. Jacobs AL, Schar P (2012) DNA glycosylases: in DNA repair and beyond. *Chromosoma* 121: 1–20
22. Klungland A, Rosewell I, Hollenbach S, Larsen E, Daly G, Epe B, Seeberg E, Lindahl T, Barnes DE (1999) Accumulation of premutagenic DNA lesions in mice defective in removal of oxidative base damage. *Proc Natl Acad Sci USA* 96: 13300–13305
23. Chattopadhyay S, Moran RG, Goldman ID (2007) Pemetrexed: biochemical and cellular pharmacology, mechanisms, and clinical applications. *Mol Cancer Ther* 6: 404–417
24. Van Triest B, Pinedo HM, Giaccone G, Peters GJ (2000) Downstream molecular determinants of response to 5-fluorouracil and antifolate thymidylate synthase inhibitors. *Ann Oncol* 11: 385–391
25. Weeks LD, Fu P, Gerson SL (2013) Uracil-DNA glycosylase expression determines human lung cancer cell sensitivity to pemetrexed. *Mol Cancer Ther* 12: 2248–2260
26. Kunz C, Focke F, Saito Y, Schuermann D, Lettieri T, Selfridge J, Schar P (2009) Base excision by thymine DNA glycosylase mediates DNA-directed cytotoxicity of 5-fluorouracil. *PLoS Biol* 7: e91
27. Zeman MK, Cimprich KA (2014) Causes and consequences of replication stress. *Nat Cell Biol* 16: 2–9
28. Bulgar AD, Weeks LD, Miao Y, Yang S, Xu Y, Guo C, Markowitz S, Oleinick N, Gerson SL, Liu L (2012) Removal of uracil by uracil DNA glycosylase limits pemetrexed cytotoxicity: overriding the limit with methoxyamine to inhibit base excision repair. *Cell Death Dis* 3: e252
29. SenGupta T, Torgersen ML, Kassahun H, Vellai T, Simonsen A, Nilsen H (2013) Base excision repair AP endonucleases and mismatch repair act together to induce checkpoint-mediated autophagy. *Nat Commun* 4: 2674
30. Burkovics P, Hajdu I, Szukacsov V, Unk I, Haracska L (2009) Role of PCNA-dependent stimulation of 3'-phosphodiesterase and 3'-5' exonuclease activities of human Ape2 in repair of oxidative DNA damage. *Nucleic Acids Res* 37: 4247–4255
31. Bennett SE, Kitner J (2006) Characterization of the aldehyde reactive probe reaction with AP-sites in DNA: influence of AP-lyase on adduct stability. *Nucleosides Nucleotides Nucleic Acids* 25: 823–842
32. Wei S, Shalhout S, Ahn YH, Bhagwat AS (2015) A versatile new tool to quantify abasic sites in DNA and inhibit base excision repair. *DNA Repair* 27: 9–18
33. Castaing B, Fourrey JL, Hervouet N, Thomas M, Boiteux S, Zelwer C (1999) AP site structural determinants for Fpg specific recognition. *Nucleic Acids Res* 27: 608–615
34. Hegde V, Wang M, Deutsch WA (2004) Human ribosomal protein S3 interacts with DNA base excision repair proteins hAPE/Ref-1 and hOGG1. *Biochemistry* 43: 14211–14217
35. Postel EH, Abramczyk BM, Levit MN, Kyin S (2000) Catalysis of DNA cleavage and nucleoside triphosphate synthesis by NM23-H2/NDP kinase share an active site that implies a DNA repair function. *Proc Natl Acad Sci USA* 97: 14194–14199
36. Roberts SA, Strande N, Burkhalter MD, Strom C, Havener JM, Hasty P, Ramsden DA (2010) Ku is a 5'-dRP/AP lyase that excises nucleotide damage near broken ends. *Nature* 464: 1214–1217
37. Ilna ES, Lavrik OI, Khodyreva SN (2008) Ku antigen interacts with abasic sites. *Biochim Biophys Acta* 1784: 1777–1785
38. Khodyreva SN, Prasad R, Ilna ES, Sukhanova MV, Kutuzov MM, Liu Y, Hou EW, Wilson SH, Lavrik OI (2010) Apurinic/apyrimidinic (AP) site recognition by the 5'-dRP/AP lyase in poly(ADP-ribose) polymerase-1 (PARP-1). *Proc Natl Acad Sci USA* 107: 22090–22095
39. Sczepanski JT, Wong RS, McKnight JN, Bowman GD, Greenberg MM (2010) Rapid DNA-protein cross-linking and strand scission by an abasic site in a nucleosome core particle. *Proc Natl Acad Sci USA* 107: 22475–22480
40. Rieger RA, Zaika EI, Xie W, Johnson F, Grollman AP, Iden CR, Zharkov DO (2006) Proteomic approach to identification of proteins reactive for abasic sites in DNA. *Mol Cell Proteomics* 5: 858–867
41. Parikh SS, Mol CD, Slupphaug G, Bharati S, Krokan HE, Tainer JA (1998) Base excision repair initiation revealed by crystal structures and binding kinetics of human uracil-DNA glycosylase with DNA. *EMBO J* 17: 5214–5226
42. Waters TR, Gallinari P, Jiricny J, Swann PF (1999) Human thymine DNA glycosylase binds to apurinic sites in DNA but is displaced by human apurinic endonuclease 1. *J Biol Chem* 274: 67–74
43. Hill JW, Hazra TK, Izumi T, Mitra S (2001) Stimulation of human 8-oxoguanine-DNA glycosylase by AP-endonuclease: potential coordination of the initial steps in base excision repair. *Nucleic Acids Res* 29: 430–438
44. Pope MA, Porello SL, David SS (2002) *Escherichia coli* apurinic-apyrimidinic endonucleases enhance the turnover of the adenine glycosylase MutY with G: a substrates. *J Biol Chem* 277: 22605–22615

45. Pettersen HS, Sundheim O, Gilljam KM, Slupphaug G, Krokan HE, Kavli B (2007) Uracil-DNA glycosylases SMUG1 and UNG2 coordinate the initial steps of base excision repair by distinct mechanisms. *Nucleic Acids Res* 35: 3879–3892
46. Sampath H, McCullough AK, Lloyd RS (2012) Regulation of DNA glycosylases and their role in limiting disease. *Free Radic Res* 46: 460–478
47. Shukla V, Halabelian L, Balagere S, Samaniego-Castruita D, Feldman DE, Arrowsmith CH, Rao A, Aravind L (2019) HMCES functions in the alternative end-joining pathway of the DNA DSB repair during class switch recombination in B cells. *Mol Cell* 77: 384–394.e4
48. Rada C, Williams GT, Nilsen H, Barnes DE, Lindahl T, Neuberger MS (2002) Immunoglobulin isotype switching is inhibited and somatic hypermutation perturbed in UNG-deficient mice. *Curr Biol* 12: 1748–1755
49. Imai K, Slupphaug G, Lee WI, Revy P, Nonoyama S, Catalan N, Yel L, Forveille M, Kavli B, Krokan HE et al (2003) Human uracil-DNA glycosylase deficiency associated with profoundly impaired immunoglobulin class-switch recombination. *Nat Immunol* 4: 1023–1028
50. Viktorovskaya OV, Greco TM, Cristea IM, Thompson SR (2016) Identification of RNA binding proteins associated with dengue virus RNA in infected cells reveals temporally distinct host factor requirements. *PLoS Negl Trop Dis* 10: e0004921
51. Xiao Z, Chang JG, Hendriks IA, Sigurethsson JO, Olsen JV, Vertegaal AC (2015) System-wide analysis of sumoylation dynamics in response to replication stress reveals novel small ubiquitin-like modified target proteins and acceptor lysines relevant for genome stability. *Mol Cell Proteomics* 14: 1419–1434
52. Zhang J, Sun W, Ren C, Kong X, Yan W, Chen X (2019) A PolH transcript with a short 3'UTR enhances PolH expression and mediates cisplatin resistance. *Cancer Res* 79: 3714–3724
53. Barnes RP, Tsao WC, Moldovan GL, Eckert KA (2018) DNA polymerase eta prevents tumor cell-cycle arrest and cell death during recovery from replication stress. *Cancer Res* 78: 6549–6560
54. Albertella MR, Green CM, Lehmann AR, O'Connor MJ (2005) A role for polymerase eta in the cellular tolerance to cisplatin-induced damage. *Cancer Res* 65: 9799–9806
55. Mengwasser KE, Adeyemi RO, Leng Y, Choi MY, Clairmont C, D'Andrea AD, Elledge SJ (2019) Genetic screens reveal FEN1 and APEX2 as BRCA2 synthetic lethal targets. *Mol Cell* 73: 885–899 e886
56. Buisson R, Niraj J, Pauty J, Maity R, Zhao W, Coulombe Y, Sung P, Masson JY (2014) Breast cancer proteins PALB2 and BRCA2 stimulate polymerase eta in recombination-associated DNA synthesis at blocked replication forks. *Cell Rep* 6: 553–564
57. Sebesta M, Burkovics P, Juhasz S, Zhang S, Szabo JE, Lee MY, Haracska L, Krejci L (2013) Role of PCNA and TLS polymerases in D-loop extension during homologous recombination in humans. *DNA Repair* 12: 691–698
58. McIlwraith MJ, Vaisman A, Liu Y, Fanning E, Woodgate R, West SC (2005) Human DNA polymerase eta promotes DNA synthesis from strand invasion intermediates of homologous recombination. *Mol Cell* 20: 783–792
59. Henderson CJ, Wolf CR (1992) Immunodetection of proteins by Western blotting. *Methods Mol Biol* 10: 221–233
60. Leung KH, Abou El Hassan M, Bremner R (2013) A rapid and efficient method to purify proteins at replication forks under native conditions. *Biotechniques* 55: 204–206
61. Chen G, Deng X (2018) Cell synchronization by double thymidine block. *Bio Protoc* 8: e2994
62. Knijnenburg TA, Wang L, Zimmermann MT, Chambwe N, Gao GF, Cherniack AD, Fan H, Shen H, Way GP, Greene CS et al (2018) Genomic and molecular landscape of DNA damage repair deficiency across The Cancer Genome Atlas. *Cell Rep* 23: 239–254 e236
63. Li W, Xu H, Xiao T, Cong L, Love MI, Zhang F, Irizarry RA, Liu JS, Brown M, Liu XS (2014) MAGeCK enables robust identification of essential genes from genome-scale CRISPR/Cas9 knockout screens. *Genome Biol* 15: 554
64. Hart T, Chandrashekhar M, Aregger M, Steinhart Z, Brown KR, MacLeod G, Mis M, Zimmermann M, Fradet-Turcotte A, Sun S et al (2015) High-resolution CRISPR screens reveal fitness genes and genotype-specific cancer liabilities. *Cell* 163: 1515–1526